research articles Journal of proteome research

Proteomic Analysis of Hydrogen Photoproduction in Sulfur-Deprived *Chlamydomonas* Cells

Mei Chen,[†,||] Le Zhao,[†,||] Yong-Le Sun,[†,||] Su-Xia Cui,[*,‡] Li-Fang Zhang,[†] Bin Yang,[‡] Jie Wang,[§] Ting-Yun Kuang,[†] and Fang Huang[*,†]

Key Laboratory of Photobiology, Institute of Botany, Chinese Academy of Sciences, Beijing 100093, China, College of Life Sciences, Capital Normal University, Beijing 100037, China, National Center of Biomedical Analysis, Beijing, China, and Graduate University of Chinese Academy of Sciences, Beijing 100049, China

Received January 26, 2010

The green alga *Chlamydomonas reinhardtii* is a model organism to study H_2 metabolism in photosynthetic eukaryotes. To understand the molecular mechanism of H_2 metabolism, we used 2-DE coupled with MALDI-TOF and MALDI-TOF/TOF-MS to investigate proteomic changes of *Chlamydomonas* cells that undergo sulfur-depleted H_2 photoproduction process. In this report, we obtained 2-D PAGE soluble protein profiles of *Chlamydomonas* at three time points representing different phases leading to H_2 production. We found over 105 Coomassie-stained protein spots, corresponding to 82 unique gene products, changed in abundance throughout the process. Major changes included photosynthetic machinery, protein biosynthetic apparatus, molecular chaperones, and 20S proteasomal components. A number of proteins related to sulfate, nitrogen and acetate assimilation, and antioxidative reactions were also changed significantly. Other proteins showing alteration during the sulfur-depleted H_2 photoproduction process were proteins involved in cell wall and flagella metabolisms. In addition, among these differentially expressed proteins, 11 were found to be predicted proteins without functional annotation in the *Chlamydomonas* genome database. The results of this proteomic analysis provide new insight into molecular basis of H_2 photoproduction in *Chlamydomonas* under sulfur depletion.

Keywords: *Chlamydomonas reinhardtii* • sulfur-depletion • H_2 photoproduction • proteomics • two-dimensional electrophoresis • MALDI-TOF • MALDI-TOF-TOF

Introduction

Clean and renewable forms of energy are needed to ensure both environmental and economic sustainability. Hydrogen gas (henceforth referred to as H_2) is considered to be the ideal clean fuel for the future.[1] However, sustainable production of H_2 is currently challenged by the primary resources, *i.e.*, fossil fuels, which are being consumed rapidly.[2] It is therefore imperative to find alternative sources and develop efficient systems for large-scale production of H_2. H_2 production by green algae, which was first discovered by Gaffron and co-workers,[3,4] is one of the attractive approaches to producing H_2. Under anaerobic conditions, green alga such as *Chlamydomonas reinhardtii*, produce a substantial quantity of H_2 via splitting water in visible light.[5,6] This approach has advantages over other means of biological H_2 production because it uses solar energy and, most importantly, the algal cells have been reported to be the most proven and potent H_2 producers that are capable of self-proliferation using inorganic nutrients. However, the commercialization of algal H_2 photoproducing systems has lagged due to the limitations such as the oxygen sensitivity of hydrogenases that catalyze the reaction of H_2 formation,[7] and the current low efficiency of solar power conversion to H_2.[8,9] To overcome such limitations, considerable research has been conducted during the past decades to determine the structure and function of the hydrogenases[9−11] as well as the physiological characteristics of H_2 photoproduction process. A breakthrough progress was made by Melis and co-workers with the establishment of a two-stage protocol, in which O_2- and H_2-evolution reactions were temporally separated by sulfur-depletion.[12,13] The protocol not only offered an efficient method switching *Chlamydomonas* from the photosynthetic growth to photoproduction of H_2, but also provided a convenient platform for in-depth investigations into the complex processes toward H_2 photoproduction. Indeed, a substantial number of experiments have been carried out based on this protocol which have led to the discovery of the distinct physiological phases of H_2 photoproduction,[14−19] as well as the complex regulation of H_2 metabolism in *Chlamydomona.*[20−23]

The completion of the *Chlamydomonas* genome sequencing project in late 2007[24] started a new era in *Chlamydomonas* research. DNA-microarray analysis indicated that more than 100 genes were up- or down-regulated throughout the process of sulfur-depleted H_2 photoproduction.[25] These findings had

* Corresponding authors. F.H.: e-mail, fhuang@ibcas.ac.cn; phone, +86-10-62836692; fax, +86-10-62594363. S.-X.C.: e-mail, sxcui@mail.cnu.edu.cn; phone, +86-10-68902666-ext-601; fax, +86-10-68902029.
† Key Laboratory of Photobiology, Institute of Botany.
|| Graduate University of Chinese Academy of Sciences.
‡ Capital Normal University.
§ National Center of Biomedical Analysis.

Published on Web 05/28/2010
10.1021/pr100076c

advanced our understanding of H_2 metabolism in *Chlamydomonas* at the genetic level. At the protein level, however, experimental data are still limited. Earlier experiments based on SDS-PAGE showed dramatic changes both in protein content and in expression profiles during the sulfur-depleted H_2 photoproduction processes.[12,14] In contrast to the large number of differentially expressed genes that had been detected, only a handful of chloroplast proteins were identified, mainly by immuno-blotting[26,27] or by 1D-PAGE coupled to mass spectrometry.[25] It has been observed that an incongruent expression pattern between mRNAs and proteins exists in yeast, mouse, human, and plant cells.[28−32] The question arises as to how this protein expression data is correlated with the mRNA abundance in terms of the specific cellular networks in *Chlamydomonas* under sulfur-depleted H_2 photoproduction process.

Proteomic analysis has emerged as a powerful tool to study global translational profiles for biological processes. The approach has been used to address fundamental questions in prokaryotic and eukaryotic algal cell biology, for example, the structural and functional aspects of cell compartments of unicellular cyanobacteria,[33−38] as well as the compositional and functional characteristics of *Chlamydomonas* proteome.[39] Comprehensive knowledge has been obtained through studies on the protein complexes and phosphoproteome of thylakoid membranes,[40−43] chloroplast ribosome,[44] eyespot,[45,46] Cilium,[47] and redox targets.[48−50] However, no experimental data regarding the changes in the soluble proteome of *Chlamydomonas* in the context of H_2 metabolism have been reported. In this work, we have used 2-DE and MALDI-TOF or MALDI-TOF/TOF-MS approaches to investigate the composition of soluble protein fraction from *Chlamydomonas*. Cells were collected at three time points representing the distinct phases leading to sulfur-depleted H_2 photoproduction. The dynamic changes of the soluble proteome of *Chlamydomonas* during the process were analyzed. We have identified 82 unique gene products that changed significantly in abundance based on the differential and quantitative analysis of Coomassie stained 2D-gel profiles using ImageMaster software. For a number of proteins, their changes were validated by semiquantitative RT-PCR analysis.

Materials and Methods

Chemicals and Reagents. Urea and sequencing-grade modified trypsin were obtained from Promega (Madison, WI). CHAPS, dithiothreitol (DTT), IPG buffer (pH 3−10), IPG DryTrip, iodoacetamide, and thiourea were purchased from GE Healthcare (GE Healthcare, Piscataway, NJ). CBB G250 was from Sigma (St. Louis, MO). All other chemicals and reagents used in the study were of analytical grade unless indicated otherwise.

Strain, Culture Condition, and H_2 Photoproduction via Sulfur Depletion. *C. reinhardtii* wild-type strain, CC124 (mt-) was obtained from the *Chlamydomonas* Genetics Center (Dr. E. Harris, Duke University, NC). The algal cells were photoheterotrophically cultured in Tris-acetate- phosphate (TAP) medium[51] at 25 °C under 200 $\mu E \cdot m^{-2} \cdot s^{-1}$ continuous cool-white fluorescent light. Liquid cultures were grown in E-flasks stirred with magnetic bars. Sulfur-depleted H_2 photoproduction was achieved according to Melis et al.[12] Briefly, midexponentially growing cells (about $2-5 \times 10^6$ cells mL^{-1}) were harvested by centrifugation at 2500*g* for 2 min at 25 °C. The cell pellet was suspended and washed once with sulfur-depleted TAP medium, in which sulfate compounds were replaced by their chloride counterparts. Cells were resuspended in the same medium and the concentration of chlorophyll (a and b) was determined according to Arnon.[52] The culture was transferred to a 1-L bottle (Schott type, Germany) and the cell density was adjusted to desired initial concentration of chlorophyll. The bottle was sealed with a silicon stopper perforated with a glass syringe, which was then connected to a Teflon tube. A switch used for controlling gas in or out was fitted in this tube. The gas evolved from the algae culture was conducted to an inverted water-filled buret through the tubing. H_2 gas accumulation was determined by measuring the amount of water that was displaced in an inverted graduated cylinder. Cells were harvested at different time points by centrifugation at 2500*g* and 4 °C for 5 min. Cell pellets were washed once and frozen at −70 °C.

Protein Extraction and Separation by 2-DE. Proteins were extracted from *Chlamydomonas* cells based on the published protocols[48,53] with modifications. Frozen cells were resuspended in ice-cold extraction buffer containing 50 mM Tris-HCl (pH 7.8), 10% glycerol, 2% β-mercaptoethanol, 1 mM EDTA, and 1 mM phenylmethylsulfonyl fluoride (PMSF). Cells were then disrupted by 3 cycles of freezing and thawing (freezing in liquid nitrogen and thawing in ice−water bath) followed by 10 cycles of ultrasonication at 8 s/30 s (JY92-II Ultrasonic Crasher, Ningbo Scientz Biotechnology Co., Ltd, China) on ice in the presence of PMSF. Unbroken cells were removed by centrifugation at 2500*g* and 4 °C for 5 min. The supernatant was collected and centrifuged at 15 000*g* for 45 min at 4 °C. The supernatant was then treated with 2% (w/v) streptomycin sulfate to eliminate nucleic acids. The sample was then subjected to ultracentrifugation at 60 000*g* at 4 °C for 45 min. Proteins in the supernatant were precipitated with 10% (w/v) trichloroacetic acid (TCA) in 80% (v/v) acetone at −20 °C for more than 2 h. Proteins were then pelleted by centrifugation at 6000*g* for 20 min at 4 °C. The protein pellet was washed three times with cold acetone and neutralized by washing twice with 5 mM ammonium bicarbonate. The pellet was dried under vacuum (SpeedVac concentrator, Savant, Holbrook, NY) and kept at −20 °C.

The dried protein pellet (ca. 1−1.5 mg) was solubilized in 500 μL of electrofocusing solution containing 7 M urea, 2 M thiourea, 4% (w/v) CHAPS, 50 mM DTT, 0.5% (v/v) IPG Buffer (pH 3−10, GE Healthcare), and a trace of bromophenol blue. The mixture was incubated at room temperature for 1 h and then sonicated in the presence of PMSF. After centrifugation at 10 000*g* for 10 min, the supernatant was transferred to a clean tube and protein concentration was determined according to Bradford method[54] with modifications to alleviate interference of detergent and reducing agents as described previously.[53]

For 2-DE of the soluble proteins, 500 μg of proteins was applied onto a linear immobilized pH gradient strip (pH 4−7, 18 cm, Amersham Biosciences). Rehydration loading and IEF were performed as described by Huang et al.[34] The IEF was carried out at 20 °C and the running program was 300 V for 40 min, 500 V for 40 min, 1000 V for 1 h, and 10 000 V until a total of 80 000 Vh was reached. Following the two-step equilibration, the second-dimension separation was carried out on 12.5% SDS-PAGE gel prepared according to Laemmli[55] with Protean II xi cell (Bio-Rad, CA) running at 20 mA/gel. Proteins were detected by Coomassie Brilliant Blue G-250 staining. 2-DE was repeated at least three times using protein samples prepared from independent experiments.

Image Analysis of 2-D Gels. 2-D gels were scanned using a UMAX PowerLook 2100XL scanner (Willich, Germany) at a

resolution of 300 dpi. 2-D gel images were analyzed with ImageMaster 2D Platinum version 5.0 (GE Healthcare). After spot detecting and editing, a scatter plot was performed according to the manufacturer's instruction (GE Healthcare) to verify reproducibility of 2D-gels from different experiments. As described previously,[53,56] relative quantification of each matched spot represented as volume% {= (volume of each spot)/(volume of total spots) × 100%}in one gel (*X*-axis) was plotted against with that in the matched CBB-stained gel (*Y*-axis). All intensive spots were excised and subjected to MS identification. Gel images from control (0 h) and sulfur-depleted cells (24 h, 32 h) were compared. Protein spots showing 2-fold or above changes in abundance were defined as being differentially expressed.

Protein Identification by Mass Spectrometry. MALDI-TOF and MALDI-TOF/TOF analysis was performed on a mass spectrometry instrument Ultraflex III from Bruker Daltonics (Bremen, Germany). Excision of protein spots and sample preparation for MALDI-TOF analysis were done as described by Huang et al.[34] For acquisition of mass spectra, 0.5 μL of samples was spotted onto a MALDI plate, followed by 0.5 μL of matrix solution (4 mg/mL α-cyano-4-hydroxycinnamic acid in 35% acetonitrile (ACN) and 1% TFA). Mass data acquisitions were piloted by flexcontrol Software v3.0 using batched-processing and automatic switching between MS and MS/MS modes. All the MS survey scans were acquired over the mass range 700−5500 m/z in the reflectron positive-ion mode and accumulated from 2000 laser shots with acceleration of 23 kV. The MS spectra were externally calibrated using PeptideCalibStandard II (Bruker Daltonics) (1046.542, 1296.685, 1347.735, 1619.822, 2093.086, 2465.198, and 3147.471) and resulted in mass errors of less than 50 ppm. The MS peaks were detected on minimum S/N ratio ≥20 and cluster area S/N threshold ≥25 without smoothing and raw spectrum filtering. Peptide precursor ions corresponding to contaminants including keratin and the trypsin autolytic products were excluded in a mass tolerance of ±0.2 Da. The filtered precursor ions with a user-defined threshold (S/N ratio ≥50) were selected for the MS/MS scan. Fragmentation of precursor ions was performed using LIFT positive mode. MS/MS spectra were accumulated from 4000 laser shots. The MS/MS peaks were detected on minimum S/N ratio ≥3 and cluster area S/N threshold ≥15 with smoothing. Mass spectra were evaluated using FlexAnalysis software. Database searching for protein identification was performed using Mascot (http://www.matrixscience.com) using the NCBI database. Search parameters allowed for mass accuracy of ±50 ppm, one miscleavage of trypsin, oxidation of methionine, and carbamidomethylation of cysteine. Proteins were identified as the highest ranking results deduced by searching in the databases of NCBInr 20080210 against other green plant. The subcellular location of proteins was predicted using TargetP program (http://www.cbs.dtu.dk/services/TargetP/).[57]

Total RNA Isolation and RT-PCR. Total RNA was isolated from *Chlamydomonas* cells using TRIzol reagent and SiMax membrane spin columns Tiangen Biotech Co., China) according to the manufacturer's protocol. Residual DNA in RNA preparations was eliminated by digestion with RNase-free DNase I (Takara). Semiquantitative RT-PCR was carried out as previously described.[58,59] Reverse transcription reactions were carried out using Oligo(dT) primers and Quant Reverse Transcriptase (Tiangen Biotech Co., China). To detect possible DNA contamination, control reactions were performed without RT. Reverse transcription products were amplified by PCR and analyzed by electrophoresis on 1.5% (w/v) agarose gels. The transcripts selected for this study include: *HYDA2* (accession no. XM_001694451), *FBP1* (accession no. XM_001690820), *FNR1* (accession no. DS496140); *PSBO* (accession no. XM_001694647); *PSBP1* (accession no. XM_001694074); *PSBP3* (accession no. XM_001690982); *EIF3I* (accession no. XM_001693214); *EIF4E* (accession no. XM_001693183); *EFG2* (accession no. XM_001703163); *RPPO* (accession no. XM_001697008); *RACK1* (accession no. XM_001698013); *HSP70B* (accession no. X96502); *CPN60C* (accession no. XM_001691301); *CYN20-2* (accession no. XM_001693889); *CYN38* (accession no. XM_001691982); *ADH1* (accession no. XM_001703533); *TPIC* (accession no. XM_001689983); *CND1b* (accession no. XM_001696829); *MDH1* (accession no. XM_001693066); *IPY1* (accession no. XM_001702525); *ARS1* (accession no. XM_001692070); *ECP88* (accession no. XM_001693996); *SAH1* (accession no. XM_001693287); *AAD1* (accession no. XM_001693127); *ICL1* (accession no. XM_001695279); *PRX1* (accession no. XM_001696559); *PRX2* (accession no. XM_001699608); *PRX5* (accession no. XM_001689403); *CCPR1* (accession no. XM_001697594), and *FAP24* (accession no. XM_001701637). The primer sequences were listed in Supporting Information Table 3. The *18s rRNA* (accession no. AY665727) was used as a positive control.[25] The log phase of RT-PCR was determined by measuring the amounts of PCR products at different PCR cycles.

Results and Discussion

H_2 Production at Different Initial Chlorophyll Concentrations. H_2 photoproduction profiles are largely dependent on culture density measured as chlorophyll concentration at the beginning of sulfur deprivation.[60,61] To determine the optimum concentration of chlorophyll that could be used for activating the H_2 metabolism of *Chlamydomonas*, sulfur-depleted H_2 photoproduction profiles were monitored at different initial chlorophyll concentrations (ICC) ranging from 10 to 30 $\mu g \cdot mL^{-1}$. Figure 1 shows that H_2 evolution was detected for each culture after 24 h of sulfur deprivation. The maximal yield of H_2 was obtained from the culture with 20 $\mu g \cdot mL^{-1}$ of the ICC (Figure 1A). After 36 h of sulfur deprivation, the amount of H_2 evolved reached 18 mL, which was 2-fold of the amount collected from the cultures at 10 and 30 $\mu g \cdot ml^{-1}$ of the ICC (Figure 1A). The accumulation of H_2 was relatively constant from 72 to 120 h of sulfur deprivation. The overall pattern of H_2 evolution was largely consistent with the earlier observations.[26,60,62] To examine the dynamic profiles of H_2 production under sulfur-depleted condition, the rate of H_2 evolution at different ICC was compared. As shown in Figure 1B, the rate of H_2 evolution increased almost linearly during the period of 24−36 h of sulfur deprivation. The rate of H_2 evolution reached 1.2 $mL \cdot L^{-1} \cdot h^{-1}$ at 36 h of sulfur deprivation for the culture at the optimal ICC (20 $\mu g \cdot mL^{-}$), which was about 2.2- to 3.1-fold of that for the cultures at lower (10 $\mu g \cdot mL^{-1}$) and higher (30 $\mu g \cdot mL^{-1}$) ICC. The maximal rate of H_2 production was shown at 48 h of sulfur deprivation for the culture at the optimal ICC (Figure 1B). Kinetic profile of sulfur-depleted H_2 photoproduction involves the sequential transition through five phases: O_2 evolution, O_2 consumption, anaerobic, H_2 production, and termination.[60,63] The lower efficiency of activating H_2 metabolism in too thin culture (10 $\mu g \cdot mL^{-1}$ ICC) could be due to insufficient anaerobiosis caused by limited cell numbers. The lowest efficiency of H_2 metabolism in the too dense culture (30 $\mu g \cdot mL^{-1}$ ICC), however, could be largely due to overall reduction of photosynthetic activity resultant from the shading

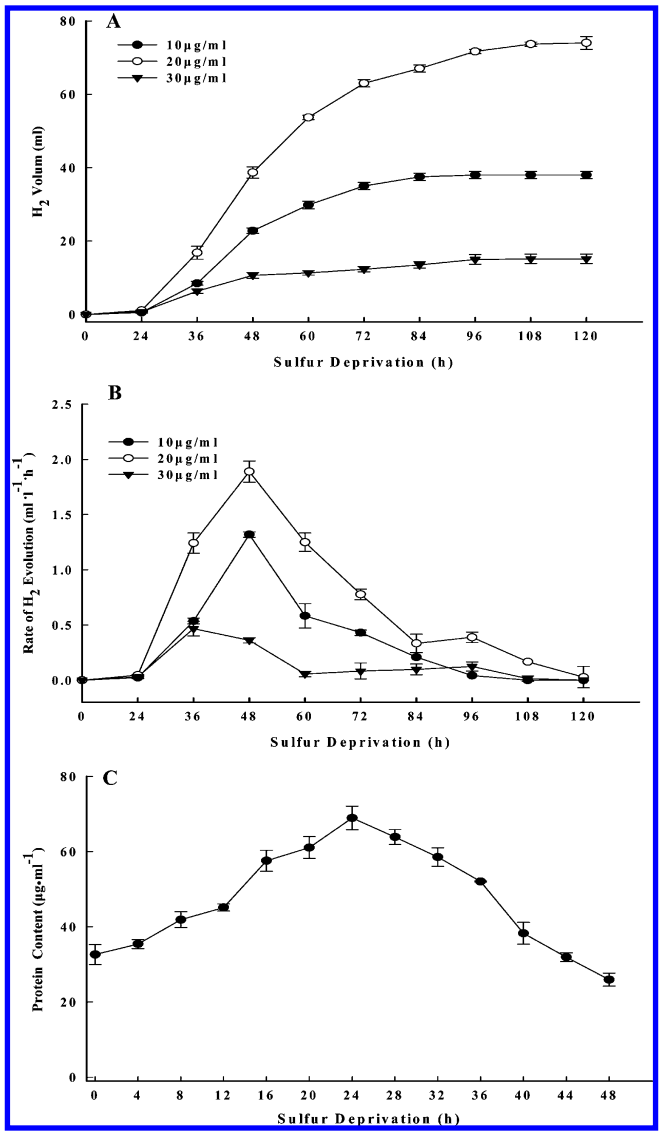

Figure 1. Time course of sulfur-depleted H_2 photoproduction in *Chlamydomonas*.. (A) Amount of H_2 produced with ICC of 10 μg/mL (●), 20 μg/mL (○), and 30 μg/mL (▼). (B) Rate of H_2 production with ICC of 10 μg/mL (●), 20 μg/mL (○), and 30 μg/mL (▼). (C) Changes in protein content of the culture with the optimal ICC during sulfur-depleted H_2 photoproduction. Measurements were performed in at least three independent experiments.

effects.[60,61] To determine the sampling time points for proteomic investigations, protein contents were estimated for the culture with the optimal ICC (20 $\mu g \cdot mL^{-1}$) within 48 h of sulfur deprivation (Figure 1C). As observed, the accumulation of total proteins gradually increased and reached its maximum level (~68 $\mu g \cdot mL^{-1}$) at 24 h of sulfur deprivation. The peak of protein content at 24 h of sulfur deprivation was correlated with the time point of initial H_2 production observed in the present investigation (Figure 1A). The observation was also in agreement with the earlier publications.[12,14,60,64] As shown in Figure 1C, the total protein content declined after 24 h of sulfur depletion. At 48 h, only about 40% of the maximal level of protein content was retained. Since the protein content at 32 h (~60 $\mu g \cdot mL^{-1}$) was slightly lower than the level at 24 h (~68 $\mu g \cdot mL^{-1}$) while the rate of H_2 evolution at this time point (32 h) was comparable to the rate at 72 h (Figure 1B and C), it was therefore determined to collect the *Chlamydomonas* cells at

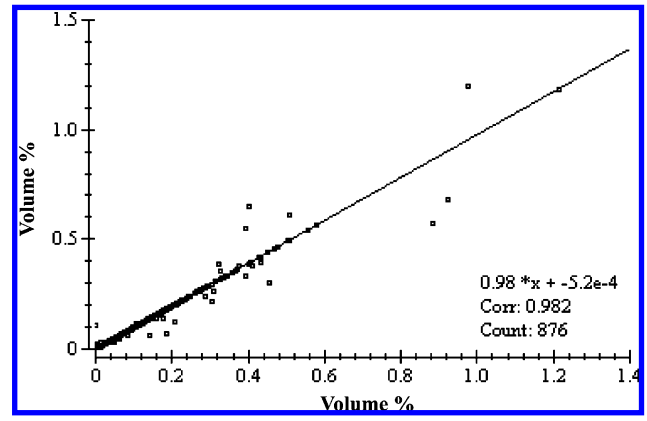

Figure 2. Scatter plot analysis between two 2-DE maps of the *Chlamydomonas* (32 h of sulfur depletion) from two independent experiments. Spot values (volume%) of the 876 matched spots were used as parameters in the analysis. The *X*-axis indicates the spot values in the 2-DE map from the first experiment, and the *Y*-axis indicates the spot values in the 2-DE map from the second experiment.

three different time points of sulfur deprivation, *i.e.*, 0, 24, and 32 h, representing the peak O_2, zero O_2, and mid H_2, respectively, for proteomic analysis.

2D-PAGE and Identification of Chlamydomonas Proteins. To investigate the proteome of the soluble protein fraction, we used the combination of 2-DE and mass spectrometry analyses. To achieve optimal separation of *Chlamydomonas* proteins by 2-DE, we tested several protein extraction/precipitation protocols, including the chloroform/methanol,[65] the phenol–methanol,[66] and the TCA/acetone.[67] The TCA/acetone method yielded highest number of protein spots with best resolution and was therefore used for constructing the 2D-maps. Protein samples prepared by this procedure were solubilized and separated by 2D-PAGE electrophoresis. More than 400 intensive spots were reproducibly detected on the gels by Coomassie Brilliant Blue (CBB) staining. To prove the reproducibility of the 2-D gels across different experiments, a scatter plot analysis was performed using ImageMaster 2D Platinum (version 5.0, GE Healthcare). Figure 2 represents scatter plot analysis of matched 2D-maps of 32 h from independent experiments. The 2D-map from the first experiment was set as a reference. After matching the 2D-maps from the second and third experiments to the reference, the scatter plot analysis was carried out using ImageMaster 2D Platinum software. The correlation coefficients between the reference and the second and third 2D-maps were 0.982 (Figure 2) and 0.968, respectively, for the gels at 32 h. Scatter plot was applied in parallel for the gels at 0 and 24 h of sulfur depletion. The average coefficients were 0.979 and 0.966 for the gels at 0 and 24 h, respectively (data not shown). These results indicate that the technical reproducibility of sample preparation and separation by 2-D gels from different experiments is sufficiently high to yield essentially identical results. Comparison of the protein patterns revealed significant differences in the intensity of a number of spots from the three biological replicates. Since the 2D-gels with proteins from cells collected at 32 h of sulfur deprivation produced more detectable protein spots than those from other two time points (0 h, 24 h), the 2D-gel image of 32 h was used as the basic 2D-map of soluble protein fraction of *Chlamydomonas*. To obtain an overall picture of the proteins identified in the present work, 27 additional spots reproducibly detected on 2D-gels (either 0

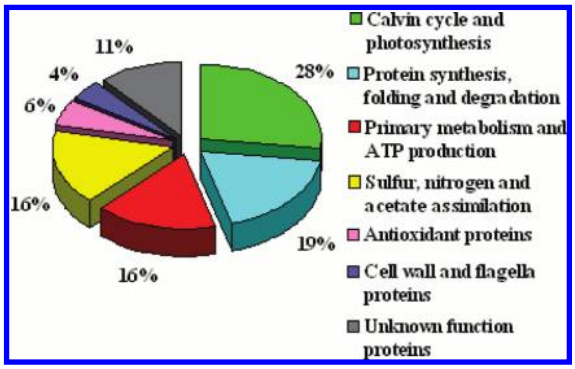

Figure 3. Distribution of identified proteins related to biological processes. A total of 159 spots representing 95 different proteins were classified.

or 24 h) were also included and indicated on the basic 2D-gel (32 h) as shown in Supplemental Figure 1. Over 250 Coomassie-stained protein spots were manually excised and subjected to protein identification. A total of 159 protein spots were identified using peptide mass fingerprints (PMF) obtained by MALDI-TOF MS coupled to protein database search. Among them, the identification of 21 proteins was confirmed by combining PMF and sequence tag by MALDI-TOF/TOF MS. The identified protein spots correspond to 95 unique gene products as shown in Supplemental Figure 1 and summarized in Supplemental Table 1. In contrast with earlier proteomic data obtained by 2D-gels,[48,68] a greater number of proteins involved in various metabolic pathways were identified in the present investigation. This achievement could be largely due to the updated information of genomic sequences of *Chlamydomonas*.[24]

Figure 3 shows the distribution of all proteins identified in this work. As expected, proteins involved in photosynthesis and energy production/conversion processes dominated (~44%) among the identified proteins. This is in agreement with the portion of chloroplast (~40%) and mitochondria (1−3%) in *Chlamydomonas*[69] as well as the general pattern of *Chlamydomonas* revealed by shotgun proteomic analysis using LC/MS technology.[70] Enzymes or proteins involved in other cellular processes, such as protein biosynthesis, inorganic assimilation, and antioxidant responses, together account for 45% of the identified proteins. In addition, we found that 11% of the proteins identified in the present work are currently annotated as hypothetical or predicted proteins due to lack of sequence similarity to any other proteins with known function. The functional significance of these novel proteins in *Chlamydomonas* remains to be elucidated. Apart from those mentioned above, our data also showed that approximately 35% of the identified proteins exhibited distinct isoforms shifted with p*I* and/or molecular mass (Supplemental Table 1). This is probably due to post-translational modifications. Further study is needed to clarify the nature of modifications as well as their functional basis for individual isoforms.

Proteomic Changes during Sulfur-Depleted H_2 Photoproduction. In total, 105 identified protein spots displayed a significant alteration in abundance during the 32 h of sulfur depletion (Figure 4), corresponding to 82 unique gene products. Their functional categories and fold changes in comparison with their level at 0 h of sulfur deprivation were summarized in Table 1. To confirm the proteomics data, a semiquantitative RT-PCR analysis was carried out using total RNA isolated from *Chlamydomonas* collected at 0, 24, and 32 h of sulfur deprivation (Figure 5). Thirty genes in total were selected for the

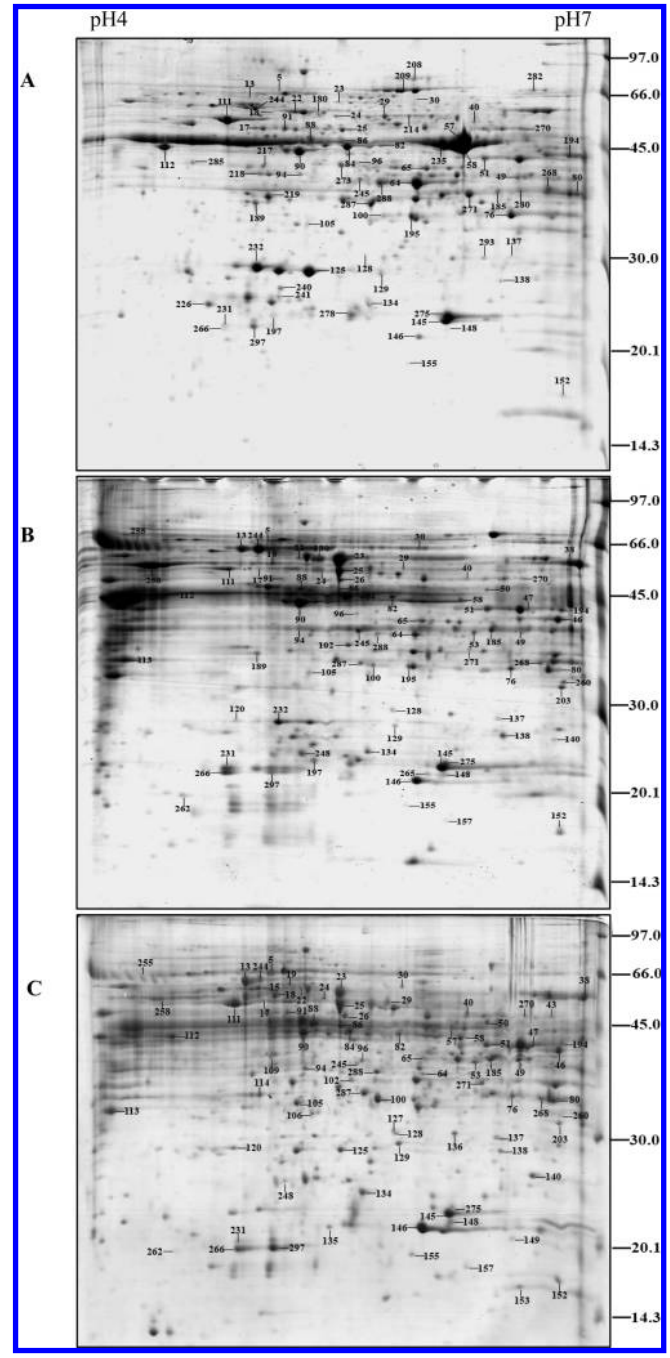

Figure 4. CBB-stained 2-D gel maps of *Chlamydomonas* soluble proteins. Cells were harvested at 0 h (A), 24 h (B), and 32 h (C) of sulfur deprivation. Identified spots were labeled according to the numbers in Table 1.

analysis. As can be seen in Figure 5, 24 transcripts showed similar kinetic changes to those observed in 2D-gel analyses (see Table 1). The gene encoding HYDA2 was included in the RT-PCR analysis because of its importance for catalyzing the reaction of H_2 formation. Clearly, the expression of *HYDA2* was up-regulated in the duration of sulfur-depleted H_2 photoproduction (Figure 5). As for *PsbO* (encoding OEE1), the correlation between RNA and protein appeared isoform-specific. For example, a close correlation between RNA and protein was found only on the isoforms represented by spots 125 and 226 (Figures 4 and 5). However, transcripts of *HSP70B*, *SAH1*, *AAD1*, *PRX1*, and *ICL1* showed opposite trends. The discrepancies

Table 1. Differentially Expressed Proteins Identified during Sulfur-Depleted H_2 Photoproduction in *Chlamydomonas*

spot no.	protein ID	gene	protein name	fold change 0 h	fold change 24 h	fold change 32 h	correlation with mRNA[a]
			Calvin Cycle and Photosynthesis				
57	NP_958405	RBCL	Rubisco large subunit	1	n.d.[b]	0.25[c]	
235			Rubisco large subunit	1	n.d.	n.d.	
153	1GK8_I	RBCS-1	Rubisco small chain I	n.d.	n.d.	0.14[d]	
157	P16137	RBCS-4	Rubisco small chain 4, chloroplast precursor	n.d.	0.02	0.14	
217	XP_001690872	FBP1[e]	Fructose-1,6-bisphosphatase	1	n.d.	n.d.	+
64	XP_001694038	PRK1	Phosphoribulokinase	1	0.36	0.12	
288			Phosphoribulokinase	1	0.45	0.89	
138	XP_001691071	RPE1	Ribulose phosphate-3-epimerase, chloroplast precursor	1	6.39	2.92	
268	EDP00292	FNR1[e]	Ferredoxin-NADP reductase	1	0.49	0.28	+
50	XP_001696881	GND1b[e,f]	6-phosphogluconate dehydrogenase, decarboxylating	n.d.	0.09	0.21	+
203	XP_001690084		6-phosphogluconolactonase-like protein	n.d.	0.52	0.16	
260	XP_001690084		6-phosphogluconolactonase-like protein	n.d.	0.13	n.d.	
125			OEE1 of photosystem II	1	n.d.	0.77	
226			OEE1 of photosystem II	1	n.d.	n.d.	
231	XP_001694699	PSBO[e,f]	OEE1 of photosystem II	1	4.27	1.73	−
232			OEE1 of photosystem II	1	1.28	n.d.	
266			OEE1 of photosystem II	1	2.5	0.88	
145			OEE2, chloroplast precursor	1	2.14	2.07	
146	P11471	PSBP	OEE2, chloroplast precursor	1	6.47	13.9	
148			OEE2, chloroplast precursor	1	4.89	4.47	
275	XP_001694126	PSBP1[e,f]	OEE2 of photosystem II	1	0.28	0.19	+
278			OEE2 of photosystem II	1	n.d.	n.d.	
155	XP_001691034	PSBP3	OEE2-like protein of thylakoid lumen	1	0.88	5.35	
287	XP_001698672	THI4a	Full-length thiazole biosynthetic enzyme	1	0.28	2.71	
280	XP_001699533	UROD1	Uroporphyrinogen-iii decarboxylase	1	n.d.	n.d.	
			Protein Synthesis, Folding, and Degradation				
82	XP_001693266	EIF3I[e]	Eukaryotic initiation factor	1	1.89	2.5	+
240	XP_001693235	EIF4E[e]	Eukaryotic initiation factor	1	n.d.	n.d.	+
102	XP_001703164	RB38	Chloroplast-targeted RNA-binding protein	n.d.	0.18	0.13	
209	XP_001703215	EFG2[e]	Elongation factor 2	1	n.d.	n.d.	+
76	XP_001697060	RPP0[e]	Acidic ribosomal protein P0	1	1.75	6.13	+
113	XP_001698065	RACK1[e]	Receptor of activated protein kinase C 1	n.d.	0.27	0.23	+
17	XP_001690281	HSP22F	Hsp 22F	1	0.3	1.06	
15				n.d.	n.d.	0.23	_
18	CAA65356	HSP70B[e]	Hsp 70B	1	7.14	9.64	
24	XP_001694468	HSP70C	Hsp 70C	1	0.83	0.25	
19	XP_001701884	BIP2	Binding protein 2	n.d.	n.d.	0.09	
91	XP_001703692	CPN60A	Chaperonin 60A	1	0.3	0.94	
26	XP_001691353	CPN60C[e]	Chaperonin 60C	n.d.	0.09	0.18	+
149	XP_001693941	CYN20−2[e]	Peptidyl-prolyl cis−trans isomerase, cyclophilin-type	n.d.	n.d.	0.07	+
189	XP_001692034	CYN38[e]	Peptidyl-prolyl cis−trans isomerase, cyclophilin-type	1	0.5	n.d.	+
112	XP_001689661	CRT2	Calreticulin 2, calcium-binding protein	1	0.25	0.61	
285			Calreticulin 2, calcium-binding protein	1	n.d.	n.d.	
293	XP_001691878	RAN1	Ran-like small GTPase	1	n.d.	n.d.	
120	XP_001701305	POA2	20S proteasome α subunit B	n.d.	0.06	0.17	
135	XP_001702638	POA3	20S proteasome α subunit C	n.d.	n.d.	0.09	
136			20S proteasome α subunit C	n.d.	n.d.	0.08	
128	XP_001690302	POA7	20S proteasome α subunit G	1	1.73	2.62	
241	XP_001693037	PBA2	20S proteasome β subunit A2	1	n.d.	n.d.	
			Primary Metabolism and ATP Production				
5	XP_001703585	ADH1[e]	Dual function alcohol dehydrogenase/acetaldehyde dehydrogenase	1	5.5	11.1	+
49	XP_001699523	PGK1	Phosphoglycerate kinase	1	2.02	9.33	
208	XP_001696348	PYC1	Pyruvate carboxylase	1	n.d.	n.d.	
129	XP_001690035	TPIC[e]	Triose phosphate isomerase	1	1	2.13	+
114	XP_001699209	PDH1b	Pyruvate dehydrogenase E1 β subunit	n.d.	n.d.	0.23	
195	XP_001693118	MDH1[e]	Malate dehydrogenase	1	0.47	n.d.	+
105	XP_001702577	IPY1[e]	Inorganic pyrophosphatase	1	2.25	7	+
270	XP_001694963	PCK1	Phosphoenolpyruvate carboxykinase	1	0.28	0.75	
282	XP_001692042	GLH1	Glycoside-hydrolase-like protein	1	n.d.	n.d.	
152	XP_001701760		6,7-dimethyl-8-ribityllumazine synthase	1	12.5	11.88	
94	XP_001690101	IRK2	Inwardly rectifying potassium channel	1	2	2.57	
84	NP_958406	ATPA	ATP synthase CF1 α subunit	1	0.55	0.4	
90	P06541	ATPB	ATP synthase F1 sector subunit β	1	1.54	0.46	
111	XP_001691632	ATP2	β subunit of mitochondrial ATP synthase	1	0.28	2.19	
29	XP_001698410	ATPvA1	Vacuolar ATP synthase, subunit A	1	0.3	2.25	
			Sulfate, Nitrogen, and Acetate Assimilation				
38			Periplasmic arylsulfatase	n.d.	1	0.75	
258	XP_001692122	ARS1[e]	Periplasmic arylsulfatase	n.d.	0.87	0.15	+
180			Periplasmic arylsulfatase	1	5.83	n.d.	
23	XP_001695509	ECP76[f]	Extracellular polypeptide Ecp76	1	24.44	12.22	+
25			Extracellular polypeptide Ecp76	1	10.67	12.08	
13	XP_001694048	ECP88[e,f]	Extracellular polypeptide Ecp88	1	10.75	10	+
244			Extracellular polypeptide Ecp88	1	6	1.35	

Table 1. Continued

spot no.	protein ID	gene	protein name	fold change 0 h	fold change 24 h	fold change 32 h	correlation with mRNA[a]
86	XP_001693339	SAH1[e]	S-adenosyl homocysteine hydrolase	1	4.5	8	−
43	XP_001701253	SUOX1	Sulfite oxidase	n.d.	n.d.	0.08	
100	XP_001691936	OASTL4	Cysteine synthase	1	1.42	4.25	
40	XP_001693179	AAD1[e]	Acetohydroxyacid dehydratase	1	3.42	8.42	−
88	XP_001703358	SBD1[f]	Selenium binding protein	1	2.12	3.41	+
273	XP_001702934	METE	Cobalamin-independent methionine synthase	1	n.d.	n.d.	
271	XP_001693042	GLN2	Glutamine synthetase	1	0.08	0.46	
53	XP_001695331	ICL1[e,f]	Isocitrate lyase	n.d.	0.2	0.23	−
185			Isocitrate lyase	1	9.4	4	
214	XP_001696603	LEU2	Isopropylmalate synthase	1	n.d.	n.d.	
47	XP_001700262	AIH2	Agmatine iminohydrolase	n.d.	0.1	0.22	
			Antioxidant Proteins				
248	CAC19677	PRX1[e]	2-cys peroxiredoxin, chloroplastic	n.d.	0.3	0.07	−
134	XP_001699660	PRX2[e]	2-cys peroxiredoxin	1	1.89	3.56	+
265			2-cys peroxiredoxin	n.d.	0.08	n.d.	
219	XP_001689455	PRX5[e]	Peroxiredoxin, type II	1	n.d.	n.d.	−
197	ABA01158		Chloroplast thioredoxin peroxidase	1	2.29	n.d.	
140	AAB04944		Superoxide dismutase precursor	n.d.	0.03	0.29	
137	XP_001697646	CCPR1[e]	Cytochrome c peroxidase	1	1.5	11.55	+
			Cell Wall and Flagellum Proteins				
22	XP_001696684		Cell wall protein	1	0.24	0.56	
255			Cell wall protein	n.d.	0.65	0.14	
96	XP_001701689	FAP24[e]	Flagellar associated protein	1	0.8	2.6	−
245			Flagellar associated protein	1	5.83	0.66	
			Unknown Function Proteins				
46	XP_001692429		Predicted protein	n.d.	0.62	0.39	
51			Predicted protein	1	3.19	2.25	
30	XP_001702190		Hypothetical protein, CHLREDRAFT_82920	1	1	19.67	
58	XP_001696473		Hypothetical protein, CHLREDRAFT_126754	1	0.27	1.77	
65	XP_001699126		Hypothetical protein, CHLREDRAFT_139416	1	0.91	0.2	
80	XP_001701585		Hypothetical protein, CHLREDRAFT_122688	1	0.45	1.02	
106	XP_001701734		Predicted protein	n.d.	n.d.	0.15	
109	XP_001696868		Hypothetical protein, CHLREDRAFT_184895	n.d.	n.d.	0.07	
218			Hypothetical protein, CHLREDRAFT_184895	1	n.d.	n.d.	
127	XP_001692807		Predicted protein	n.d.	n.d.	0.08	
194	XP_001692545		Predicted protein	1	1.44	n.d.	
262	EDO96768		Predicted protein	n.d.	0.08	0.06	
297	XP_001693241		Hypothetical protein, CHLREDRAFT_205900	1	n.d.	n.d.	

[a] +, correlated; −, not correlated. [b] Not detected. [c] Fold change in comparison with the value of volume% on 2D-gels at 0 h. [d] Value of volume% on 2D-gels. [e] Comparison with the data from Figure 5. [f] Comparison with the data from Nguyen et al.[25]

between the RNA change and protein change could be due to the differences in their kinetics of accumulation or turnover under the current experimental conditions.

The largest group of differentially expressed proteins consists of proteins involved in photosynthesis (25 spots). The second largest group was attributed to the components of protein biosynthesis and quality control pathways (23 spots). The third group included the proteins related to primary metabolism and ATP production (15 spots). Significant changes were also observed for numerous proteins involved in sulfur metabolism and oxidative reactions. In addition, 11 of the differentially proteins were hypothetical or predicted proteins with unknown function. The physiological implications of the proteins are discussed below.

Calvin Cycle and Photosynthesis. As mentioned, the largest group of proteins differentially expressed under sulfur-depleted H_2 photoproduction are those involved in photosynthesis. The protein level of Rubisco, a key enzyme of Calvin cycle for CO_2 assimilation, was previously shown to decrease dramatically during sulfur-depleted H_2 photoproduction process.[14] Similarly, 3 protein components in Calvin cycle, *i.e.*, Rubisco large subunit (spots 57, 235), phosphoribulokinase (spots 64, 288), and fructose-1, 6-bisphosphatase (encoded by *FBP1*, spot 217) were found to be reduced significantly in the duration of H_2 production (Figure 4, Table 1). Since these enzymes catalyze the irreversible reactions in Calvin cycle, the observed decreased levels of these enzymes along with the decrease in both protein and mRNA levels of ferredoxin-NADP reductase (spot 268) strongly suggested that the Calvin cycle was impaired under sulfur-depleted conditions. In contrast, the protein levels of three enzymes involved in pentose phosphate pathway, *i.e.*, 6-phosphogluconate dehydrogenase (spot 50), 6-phosphogluconolactonase-like protein (spots 203, 260), and the chloroplast precursor of phosphate-3-epimerase (spot 138) apparently increased or induced during sulfur-depleted H_2 production (Table 1). Compared to that at 0 h, the level of chloroplast precursor of phosphate-3-epimerase increased 6.4- and 2.9-fold at 24 and 32 h of sulfur depletion, respectively (Figure 4, Table 1). Induction of 6-phosphogluconate dehydrogenase (Figure 4) was in good agreement with its up-regulated gene expression detected in the present experiment using RT-PCR analysis (Figure 5) as well as in the previous DNA microarray investigation.[25] Taken together, the data implies that pentose phosphate pathway is activated while Calvin cycle is inactivated during sulfur-depleted H_2 photoproduction in *Chlamydomonas*.

Dramatic changes were not restricted to the proteins involved in photosynthetic dark reactions. In terms of differentially expressed proteins involved in light reaction of photo-

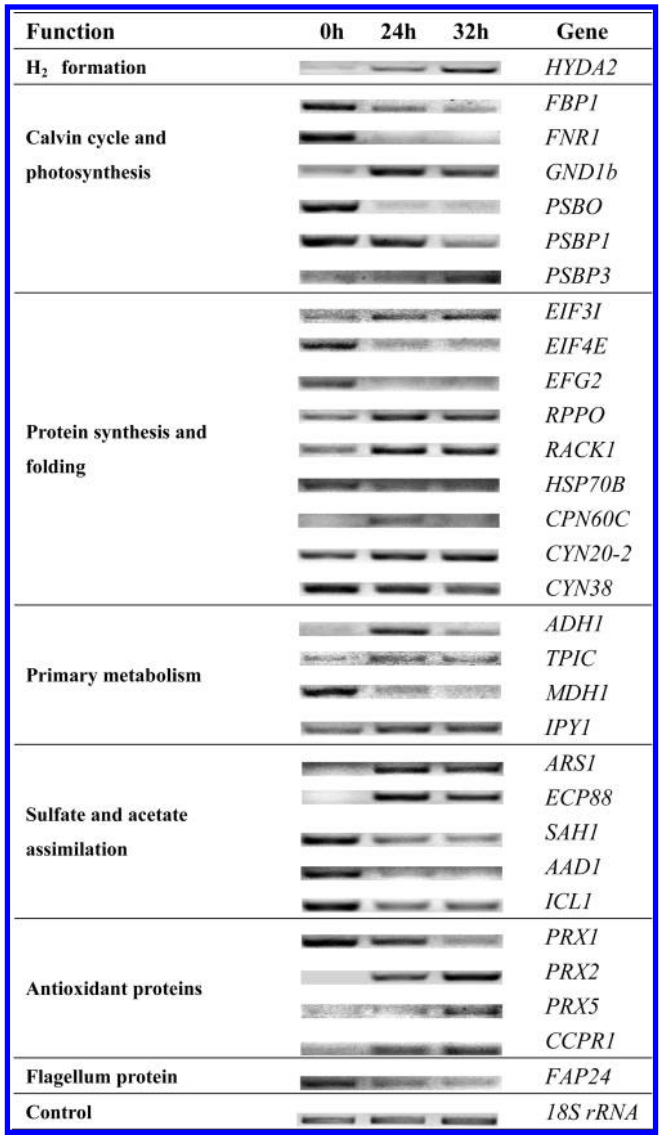

Figure 5. RT-PCR analysis of selected proteins identified by 2-DE. Expression of *18S rRNA* was used as an internal reference. All RT-PCR experiments were repeated twice, and the similar results were obtained.

synthesis, we found that OEE1 (encoded by *PsbO*) showed complex patterns depending on the individual isoforms of the protein (spots 125, 226, 231, 232, 266). OEE1 is the only extrinsic subunit of PSII present in all oxygenic organisms.[71] Under normal growth condition, OEE1 had been proposed as a buffering network providing efficient acceptors of protons derived from substrate water molecules.[72] The precise role of OEE1 under sulfur-depleted H_2 photoproduction, however, remains unclear. In this work, we have evidenced multiple isoforms of OEE1 represented by 12 distinct spots (Supplemental Table 1); five of them displayed a remarkable change in abundance (Figure 4, Table 1). This observation indicates that post-translational modifications of OEE1 may have occurred during the process. We propose that the modifications of protein and the changes in abundance of the isoforms take an important part in the transformation of cellular metabolism of *Chlamydomonas* from normal photosynthetic growth to H_2 evolution under such condition.

The *Chlamydomonas* genome contains 7 genes that encode PsbP-like proteins. Interestingly, OEE2 proteins encoded by *PsbP1* and *PsbP3*, respectively, showed opposite trends during sulfur-depleted H_2 photoproduction. Down-regulated gene expression of *PsbP1* was previously detected by DNA microarray analysis.[25] In the present work, we have observed apparent decline in both protein (spots 275, 278) and mRNA levels of *PsbP1* based on 2D-gels and RT-PCR analysis (Figures 4 and 5). In contrast, protein levels of its precursor forms (spots 145, 146, 148) were found accumulated 2.1- to 13.9-fold during H_2 production stages (Figure 4, Table 1). This strongly suggested that the translocation and/or processing of pre-OEE2 encoded by *PsbP* may have been affected under sulfur-depleted H_2 photoproduction. On the other hand, our data showed the protein level of OEE2-like protein (encoded by *PsbP3*, spot 155) appeared increased, particularly at the 32-h time point. Although multiple *PsbP* genes are identified in the genomes of all oxyphototrophs across cyanobacteria and plants, the functional significance of OEE2 proteins in different photosynthetic organisms including *Chlamydomonas* is poorly understood.[73] The finding of the presence of various isoforms of OEE2 (Supplemental Table 1) as well as their changes in abundance under sulfur-depleted H_2 photoproduction (Table 1) provides important clues for further elucidation of its function.

Protein Biosynthesis and Quality Control. The second largest group of the differentially expressed proteins identified was attributed to the proteins involved in protein biosynthesis, folding and degradation (Table 1). Six of the proteins constituting the cytosolic- or plastid-translation machineries, *i.e.*, eukaryotic initiation factors (encoded by *EIF3I*, spot 82) and *EIF4E* (spot 240), elongation factor 2 (encoded by *EFG2*, spot 209), acidic ribosomal protein P0 (encoded by *RPP0*, spot 76), receptor of activated protein kinase C 1 (encoded by *RACK1*, spot 113), and chloroplast-targeted RNA-binding protein (encoded by *RB38*, spot 102), significantly changed in abundance during sulfur-depleted H_2 photoproduction process (Figure 4, Table 1). Both protein and mRNA levels of *RPP0*, *RACK1*, and *EIF3I* showed similar kinetic change and apparently increased during the H_2 production phases (Figures 4 and 5). These are the components of the cytosolic translation machinery of *Chlamydomonas*.[74] Compared to that at 0 h, the protein level of *RPP0* and *EIF3I* increased 2.5- and 6.1-fold, respectively, after 32 h of sulfur depletion. On the other hand, the levels of EFG2 (spot 209), a protein facilitating plastidic translation, and its mRNA reduced remarkably after 24 h of sulfur depletion (Figures 4 and 5). On the basis of these observations, we propose that protein biosynthesis in cytosol was stimulated to a great extent toward sulfur-depleted H_2 photoproduction in *Chlamydomonas*.

In the *Chlamydomonas* genome, 9 genes were found encoding the Hsp70-like proteins known as *Hsp70A*−*Hsp70G*, *Bip1*, and *Bip2*.[75] Our data showed that the protein levels of 3 Hsp70s (Hsp70B, spot 15 Hsp70C, spot 24; Bip 2, spot 19), two chaperonins (chaperonin 60A, spot 91; chaperonin 60C, spot 26) and the small heat shock protein Hsp22F (spot 17) were altered in the duration of H_2 photoproduction (Figure 4, Table 1). Interestingly, all the differentially expressed molecular chaperones identified in this work appeared to be the organelle-located counterparts of the protein family in *Chlamydomonas*.[76] Among these Hsp70s, Hsp70B and Hsp70C are localized in chloroplast and mitochondria.[77,78] It has been reported that Hsp70B interacts with Vipp1,[79] a protein that was found located in plasma and thylakoid membranes of cyanobacteria[34,80] and is essential for thylakoid formation.[81] In this work, we found the chloroplast-located Hsp70B increased

Table 2. Prediction of Subcellular Location of Differentially Expressed Proteins Involved in Oxidative Stress Responses and Protein Folding in *Chlamydomonas*[a]

spot no.	gene	protein	up or down regulation during H_2 production	subcellular location
248	PRX1	2-cys peroxiredoxin, chloroplastic	Up	C[b]
134	PRX2	2-cys peroxiredoxin	Up	O[c]
265	PRX2	2-cys peroxiredoxin	Up	O
197		Chloroplast thioredoxin peroxidase	Up	C
140		Superoxide dismutase precursor	Up	M[d]
137	CCPR1	Cytochrome c peroxidase	Up	M
219	PRX5	Peroxiredoxin, type II	Down	M
18	HSP70B	Hsp 70B	Up	C
24	HSP70C	Hsp 70C	Down	M
17	HSP22F	Hsp 22F	Down	C
91	CPN60A	Chaperonin 60A	Down	C
26	CPN60C	Chaperonin 60C	Up	M[e]
149	CYN20−2	Peptidyl-prolyl cis−trans isomerase, cyclophilin-type	Up	C
189	CYN38	Peptidyl-prolyl cis−trans isomerase, cyclophilin-type	Down	M

[a] Predicted by the TargetP program at the Internet web http://www.cbs.dtu.dk/services/TargetP/. [b] Chloroplast. [c] Other. [d] Mitochondria. [e] Identified in mitochondria proteome by von Lis et al.[83]

nearly 10-fold within 32 h of sulfur deprivation (spot 18) whereas the mitochondrial-located Hsp70C (spot 24) declined gradually (Figure 4, Table 1). Considering the general role of Hsp70B in refolding of stress-denatured chloroplast proteins,[77,82] we postulate that the accumulation of Hsp70B observed in the present investigation may serve as an important module for long-term survival of the organism under sulfur-depleted condition.

On the basis of TargetP prediction[57] and homology analysis, there are four members of Hsp60s in *Chlamydomonas*.[76] In this investigation, we found that the protein levels of chaperonin 60A (spot 91), putatively located in chloroplast, and the mitochondrial-located chaperonin 60C[83] changed apparently under sulfur deprivation (Figure 4, Table 1). The present work also demonstrated, for the first time, the expression of *CYN20-2* and *CYN38* encoding cyclophilin-type peptidyl-prolyl *cis−trans* isomerases (spot 149, spot 189) in *Chlamydomonas*. Interestingly, their kinetic changes showed opposite trend, at both protein and RNA levels, under sulfur-depleted H_2 production process (Figures 4 and 5). In *Arabidopsis*, AtCYP20-2 is one of only two immunophilins with characterized peptidyl-prolyl isomerase activity in the thylakoid lumen of the chloroplast.[84] Prediction by TargetP[57] program revealed that the gene product of *CYN 20-2* is chloroplast targeted whereas *CYN 38* gene product is located in mitochondria (Table 2). Consistently, the chloroplast-located CYN 20-2 protein (spot 149) seemed induced while the mitochondria-located CYN 38 protein (spot 189) diminished under sulfur-depleted H_2 production process. Apparently, more detailed experimental work is needed to verify subcellular location of these cyclophilin-type peptidyl-prolyl *cis−trans* isomerases in *Chlamydomonas* and to specify their functional significance in H_2 metabolism under such conditions. With regard to protein degradation, all three components of 20S proteasome α subunit identified in this work (B, spot 120; C, spot 135, 136; G, spot 128) appeared induced or enhanced during sulfur-depleted H_2 photoproduction (Figure 4, Table 1). Since the 20S proteasome functions as the catalytic core of the 26S proteasome,[85] the elevated level of the components of 20 proteasome observed in the present experiments suggests that substantial rearrangements in the cellular proteome may have occurred during sulfur-depleted H_2 photoproduction process.

Primary Metabolism and ATP Production. Three enzymes involved in glycolysis were up-regulated, *i.e.*, dual function alcohol dehydrogenase/acetaldehyde dehydrogenase (spot 5), phosphoglycerate kinase (spot 49), and triose phosphate isomerase (spot 129) (Figure 4, Table 1). On the other hand, the level of 2 enzymes involved in TCA cycle, *i.e.*, malate dehydrogenase (spot 195) and pyruvate carboxylase (spot 208), was lower than that at 0 h (Figure 4, Table 1). RT-PCR analysis revealed similar kinetic change of the mRNA (*ADH1*, *TPIC*, *MDH1*) as their proteins (Figures 4 and 5). These observations suggest that fermentative metabolism was stimulated whereas TCA cycle was repressed at the H_2 photoproduction phases. Moreover, variation in the level of several subunits of ATP synthases, *i.e.*, α- and β-subunits of CF1 ATP synthase (spot 84, 90), β-subunit of mitochondrial ATP synthase (spot 111), and A subunit of vacuolar ATP synthase (spot 29), was apparent throughout the measured period (Figure 4, Table 1). The overall level of the α- and β-subunits of CF1 ATP synthase declined about 50% in the duration of H_2 photoproduction. Since both subunits are peripheral CF1 complex proteins located in the stromal side of the thylakoid membrane, their dramatic reduction may indicate an uncoupling of the ATP production from the photosynthetic electron-transport chain in favor of [Fe−Fe] hydrogenase pathway under such conditions. Interestingly, the β-subunit of mitochondrial ATP synthase (spot 111) and the A-subunit of vacuolar ATP synthase (spot 29) showed a slightly different pattern in comparison with that of CF1 subunits. Compared to the level at 0 h, only about 30% was observed for the β-subunit of mitochondrial ATP synthase and the A-subunit of vacular ATP synthase at 24 h of sulfur deprivation. After 24 h, however, the level of the two proteins apparently increased rapidly and accumulated about 2.2-fold (Table 1). These changes, together with the remarkable increase in both protein and mRNA levels of inorganic pyrophosphatase (spot 105), putatively located in chloroplast of *Chlamydomonas*, may be an indication of alteration in energetic status within the organelles of *Chlamydomonas* toward H_2 production under sulfur-depleted conditions.

Sulfur, Nitrogen, and Acetate Assimilation. Three proteins involved in sulfur metabolism were up-regulated at both protein and mRNA levels. They are periplasmic arylsulfatase (encoded by *ARS1*, spots 38, 180, 258), extracellular polypeptide

Ecp76 (encoded by *ECP76*, spots 23, 25), and Ecp88 (encoded by *ECP88*, spots 13, 244) (Figures 4 and 5). This is consistent with earlier reports[25,86−88] and was proposed to be one of the specific responses to sulfur starvation.[89] In this work, we also observed elevated level of 4 proteins related to sulfur metabolism: *S*-adenosyl homocysteine hydrolase (spot 86), sulfite oxidase (spot 43), cysteine synthase (spot 100), selenium binding protein (spot 88), and acetohydroxyacid dehydratase (spot 40), an enzyme involved in biosynthesis of valine, during the 32 h of sulfur deprivation (Table 1). In addition, we found that cobalamin-independent methionine synthase (spot 273) was diminished while agmatine iminohydrolase catalyzing the conversion of agmatine into *N*-carbamoylputrescine (spot 47) was induced under sulfur-depleted conditions (Table 1). Considering their mitochondrial-location in *Chlamydomonas*,[78] we postulate that biosynthesis of putrescine, putatively taking place in mitochondria, is stimulated whereas the biosynthesis of methionine via cobalamin-independent methionine synthase is repressed in sulfur-depleted H_2 photoproduction. Apart from the proteins involved in sulfur assimilation mentioned above, we have found that the protein level of glutamine synthetase (encoded by *GLN2*, spot 271) decreased significantly under sulfur depletion (Figure 4, Table 1). This is the plastid-located isoform of glutamine synthetase that catalyzes the key reactions on incorporation of nitrogen into carbon skeletons in *Chlaymedomonas*.[90−92] Furthermore, our experimental data showed that the protein level of isocitrate lyase (encoded by *ICL1*) was either induced (spot 53) or enhanced up to 9.4-fold (spot 185) under sulfur-depleted H_2 photoproduction (Figure 4, Table 1). Since the enzyme represents one of the key enzymes in acetate assimilation through the glyoxylate pathway, the remarkable accumulation of the enzyme may indicate, at least in part, an increased consumption of acetate during the first 24 h of sulfur depletion. Indeed, earlier experiments showed that the amount of acetate in the culture medium declined by about 50% during the 0−30-h period of sulfur deprivation.[12]

Antioxidant Proteins. In this work, we found that 3 peroxiredoxins with different subcellular locations changed in abundance during surlfur-depleted H_2 production process (Figure 4, Table 1). The chloroplast-located 2-cys peroxiredoxin (encoded by *PRX1,* spot 248) and cytosol-located 2-cys peroxiredoxin (encoded by *PRX2,* spots 134, 265) were identified previously among the thioredoxin targets in *Chlamydomonas*.[49,50] Our data demonstrated that the level of these proteins increased up to 3.6-fold during sulfur-depleted H_2 production process. Type II -peroxiredoxin (encoded by *PRX5,* spot 219) was newly identified in the present work. Its location was predicted to be in mitochondria (Table 2). The level of this protein diminished under sulfur depletion (Figure 4, Table 1). Consistently, our data showed that the protein level of chloroplastic thioredoxin peroxidase (spot 197) was elevated more than 2-fold during the first 24 h of sulfur-depletion whereas remarkable accumulation of mitochondrial cytochrome c peroxidase (encoded by *CCPR1*, spot 137) was observed after 32 h of sulfur-depletion (Figure 4, Table 1). Together with the induction of the precursor of superoxide dismutase (spot 140), we postulate that hydrogen peroxide (H_2O_2) and superoxide radicals may have been the major reactive species produced in mitochondria during the prolonged period of sulfur depletion.

Cell Wall, Flagellar, and Unknown-Function Proteins. Apart from the differentially expressed proteins that are involved in distinct metabolic pathways, 17 spots corresponding to 13 different proteins (encoded by 13 unique genes) with no functional annotation also showed significant changes in their abundance during sulfur-depleted H_2 photoproduction process (Table 1). These include the putative cell wall protein (encoded by the gene (XM_001696632), spot 22, 255), the flagella-associated protein (encoded by *FAP24,* spot 96, 245), and proteins encoded by 11 unique genes that are predicted or hypothetical proteins in *Chlamydomonas* genome database (Table 1). Interestingly, two isoforms of the cell wall protein (spots 22, 255) and flagella-associated protein (spots 96, 245, encoded by *FAP24*) apparently changed in opposite trends under sulfur-depleted treatment (Table 1). For instance, the isoform of FAP24 with lower mass (spot 245) increased 5.8-fold during the first 24 h of sulfur derivation then decreased rapidly in the longer period, whereas a slight decline was observed for the other isoform (spot 96) at 24 h of sulfur derivation but increased 2.6-fold afterward (Figure 4, Table 1). Similar pattern in variation of protein levels was found for other two isoforms of hypothetical protein represented by spots 109 and 218 (Figure 4, Table 1). Seven of other predicted or hypothetical proteins were found induced or enhanced, while 3 (spots 65, 80, 297) were decreased significantly during the H_2 production phases. The correlation between their variations in abundance and H_2 photoproduction under sulfur-depleted condition provides an important clue for in-depth study of the biological function of these novel proteins.

Concluding Remarks

In summary, our present work revealed, for the first time, major and dynamic changes in the soluble proteome of *Chlamydomonas* during sulfur-depleted H_2 photoproduction. Out of the identified 159 different protein spots (Supplementary Table 1), 105 were found enhanced or reduced significantly in abundance throughout the sulfur-depleted H_2 photoproduction process, corresponding to 82 unique genes (Table 1). Our experimental data indicates that during the process of H_2 photoproduction, proteins involved in pentose phosphate pathway and fermentative metabolism were enhanced, while proteins involved in Calvin cycle and TCA cycle decreased, suggesting that coordination of different metabolic pathways is closely associated with H_2 photoproduction. Remarkably, a substantial number of enhanced or reduced proteins including the gene products encoded by *PSBO*, *PSBP*, and *ICL1* were found to be present in multiple isoforms, likely due to post-translational modifications. Furthermore, we identified more than a dozen of proteins currently annotated as hypothetical or predicted proteins in the *Chlamydomonas* genome database. These results provide not only detailed information regarding the intricate interplay between photosynthesis and respiration in switching the organism from O_2-evolving to H_2 production, but also more candidate genes for targeted genetic engineering of *Chlamydomonas* that would lead to further elucidation of fundamental mechanisms of H_2 production and its utilization in industry scale.

Acknowledgment. This work was supported by the Chinese Ministry of Sciences and Technology (grant no. 2009CB220000), the National Natural Sciences Foundation of China (grant no. 30570130) and the Chinese Academy of Sciences.

Supporting Information Available: Supplemental Figure 1, CBB-stained representative 2-DE image of C*hlamy-*

domonas soluble proteins resolved by using linear pH 4−7 IPG (18 cm) followed by SDS-PAGE (12.5%); Supplemental Figure 2, MALDI-TOF spectra of identified protein spots listed in Supplemental Table 1; Supplemental Figure 3, MALDI-TOF/TOF spectra of identified protein spots listed in Supplemental Table 1; Supplemental Table 1, summary of proteins identified from *Chlamydomonas* using 2-DE coupled with MALDI-MS; Supplemental Table 2, MALDI-TOF spectra peak list of peptides generated by tryptic digestion of identified protein spots; Supplemental Table 3, list of primers used for RT-PCR of *Chlamydomonas* genes. This material is available free of charge via the Internet at http://pubs.acs.org.

References

(1) Melis, A.; Happe, T. Hydrogen production. Green algae as a source of energy. *Plant Physiol.* **2001**, *127* (3), 740–748.

(2) RifkinJ. In *The Hydrogen Economy*; Penguin Putnam Inc.: New York, 2002; pp 64−91.

(3) Gaffron, H. Reduction of carbon dioxide with molecular hydrogen in green alga. *Nature* **1939**, *143* (3614), 204–205.

(4) Gaffron, H.; Rubin, J. Fermentative and photochemical production of hydrogen in algae. *J. Gen. Physiol.* **1942**, *26* (2), 219–240.

(5) Gfeller, R. P.; Gibbs, M. Fermentative metabolism of *Chlamydomonas reinhardtii* 0.1. analysis of fermentative products from starch in dark and light. *Plant Physiol.* **1984**, *75* (1), 212–218.

(6) Greenbaum, E. Energetic efficiency of hydrogen photoevolution by algal water splitting. *Biophys. J.* **1988**, *54* (2), 365–368.

(7) Ghirardi, M. L.; Togasaki, R. K.; Seibert, M. Oxygen sensitivity of algal H_2- production. *Appl. Biochem. Biotechnol.* **1997**, *63*−*65*, 141–151.

(8) Esper, B.; Badura, A.; Rogner, M. Photosynthesis as a power supply for (bio-)hydrogen production. *Trends Plant Sci.* **2006**, *11* (11), 543–549.

(9) Ghirardi, M. L.; Posewitz, M. C.; Maness, P. C.; Dubini, A.; Yu, J. P.; Seibert, M. Hydrogenases and hydrogen photoproduction in oxygenic photosynthetic organisms. *Annu. Rev. Plant Biol.* **2007**, *58*, 71–91.

(10) Kamp, C.; Silakov, A.; Winkler, M.; Reijerse, E. J.; Lubitz, W.; Happe, T. Isolation and first EPR characterization of the [FeFe]-hydrogenases from green algae. *Biochim. Biophys. Acta* **2008**, *1777* (5), 410–416.

(11) Winkler, M.; Kuhlgert, S.; Hippler, M.; Happe, T. Characterization of the key step for light-driven hydrogen evolution in green algae. *J. Biol. Chem.* **2009**, *284* (52), 36620–36627.

(12) Melis, A.; Zhang, L. P.; Forestier, M.; Ghirardi, M. L.; Seibert, M. Sustained photobiological hydrogen gas production upon reversible inactivation of oxygen evolution in the green alga *Chlamydomonas reinhardtii*. *Plant Physiol.* **2000**, *122* (1), 127–135.

(13) Ghirardi, M. L.; Zhang, J. P.; Lee, J. W.; Flynn, T.; Seibert, M.; Greenbaum, E.; Melis, A. Microalgae: a green source of renewable H_2. *Trends Biotechnol.* **2000**, *18* (12), 506–511.

(14) Zhang, L. P.; Happe, T.; Melis, A. Biochemical and morphological characterization of sulfur-deprived and H_2-producing *Chlamydomonas reinhardtii* (green alga). *Planta* **2002**, *214* (4), 552–561.

(15) Kosourov, S.; Seibert, M.; Ghirardi, M. L. Effects of extracellular pH on the metabolic pathways in sulfur-deprived, H_2-producing *Chlamydomonas reinhardtii* cultures. *Plant Cell Physiol.* **2003**, *44* (2), 146–155.

(16) Posewitz, M. C.; Smolinski, S. L.; Kanakagiri, S.; Melis, A.; Seibert, M.; Ghirardi, M. L. Hydrogen photoproduction is attenuated by disruption of an isoamylase gene in *Chlamydomonas reinhardtii*. *Plant Cell* **2004**, *16* (8), 2151–2163.

(17) Kruse, O.; Rupprecht, J.; Bader, K. P.; Thomas-Hall, S.; Schenk, P. M.; Finazzi, G.; Hankamer, B. Improved photobiological H_2 production in engineered green algal cells. *J. Biol. Chem.* **2005**, *280* (40), 34170–34177.

(18) Mus, F.; Cournac, L.; Cardettini, W.; Caruana, A.; Peltier, G. Inhibitor studies on non-photochemical plastoquinone reduction and H_2 photoproduction in *Chlamydomonas reinhardtii*. *Biochim. Biophys. Acta* **2005**, *1708* (3), 322–332.

(19) Antal, T. K.; Krendeleva, T. E.; Laurinavichene, T. V.; Makarova, V. V.; Ghirardi, M. L.; Rubin, A. B.; Tsygankov, A. A.; Seibert, M. The dependence of algal H_2 production on photosystem II and O_2 consumption activities in sulfur-deprived *Chlamydomonas reinhardtii* cells. *Biochim. Biophys. Acta* **2003**, *1607* (2−3), 153–160.

(20) Surzycki, R.; Cournac, L.; Peltiert, G.; Rochaix, J. D. Potential for hydrogen production with inducible chloroplast gene expression in *Chlamydomonas*. *Proc. Natl. Acad. Sci. U.S.A.* **2007**, *104* (44), 17548–17553.

(21) Kosourov, S.; Patrusheva, E.; Ghirardi, M. L.; Seibert, M.; Tsygankov, A. A comparison of hydrogen photoproduction by sulfur-deprived *Chlamydomonas reinhardtii* under different growth conditions. *J. Biotechnol.* **2007**, *128* (4), 776–787.

(22) Hemschemeier, A.; Fouchard, S.; Cournac, L.; Peltier, G.; Happe, T. Hydrogen production by *Chlamydomonas reinhardtii*: an elaborate interplay of electron sources and sinks. *Planta* **2008**, *227* (2), 397–407.

(23) Chochois, V.; Dauvillee, D.; Beyly, A.; Tolleter, D.; Cuine, S.; Timpano, H.; Ball, S.; Cournac, L.; Peltier, G. Hydrogen production in *Chlamydomonas*: photosystem II-dependent and -independent pathways differ in their requirement for starch metabolism. *Plant Physiol.* **2009**, *151* (2), 631–640.

(24) Merchant, S. S.; Prochnik, S. E.; Vallon, O.; Harris, E. H.; Karpowicz, S. J.; Witman, G. B.; Terry, A.; Salamov, A.; Fritz-Laylin, L. K.; Marechal-Drouard, L.; Marshall, W. F.; Qu, L. H.; Nelson, D. R.; Sanderfoot, A. A.; Spalding, M. H.; Kapitonov, V. V.; Ren, Q. H.; Ferris, P.; Lindquist, E.; Shapiro, H.; Lucas, S. M.; Grimwood, J.; Schmutz, J.; Cardol, P.; Cerutti, H.; Chanfreau, G.; Chen, C. L.; Cognat, V.; Croft, M. T.; Dent, R.; Dutcher, S.; Fernandez, E.; Fukuzawa, H.; Gonzalez-Balle, D.; Gonzalez-Halphen, D.; Hallmann, A.; Hanikenne, M.; Hippler, M.; Inwood, W.; Jabbari, K.; Kalanon, M.; Kuras, R.; Lefebvre, P. A.; Lemaire, S. D.; Lobanov, A. V.; Lohr, M.; Manuell, A.; Meir, I.; Mets, L.; Mittag, M.; Mittelmeier, T.; Moroney, J. V.; Moseley, J.; Napoli, C.; Nedelcu, A. M.; Niyogi, K.; Novoselov, S. V.; Paulsen, I. T.; Pazour, G.; Purton, S.; Ral, J. P.; Riano-Pachon, D. M.; Riekhof, W.; Rymarquis, L.; Schroda, M.; Stern, D.; Umen, J.; Willows, R.; Wilson, N.; Zimmer, S. L.; Allmer, J.; Balk, J.; Bisova, K.; Chen, C. J.; Elias, M.; Gendler, K.; Hauser, C.; Lamb, M. R.; Ledford, H.; Long, J. C.; Minagawa, J.; Page, M. D.; Pan, J. M.; Pootakham, W.; Roje, S.; Rose, A.; Stahlberg, E.; Terauchi, A. M.; Yang, P. F.; Ball, S.; Bowler, C.; Dieckmann, C. L.; Gladyshev, V. N.; Green, P.; Jorgensen, R.; Mayfield, S.; Mueller-Roeber, B.; Rajamani, S.; Sayre, R. T.; Brokstein, P.; Dubchak, I.; Goodstein, D.; Hornick, L.; Huang, Y. W.; Jhaveri, J.; Luo, Y. G.; Martinez, D.; Ngau, W. C. A.; Otillar, B.; Poliakov, A.; Porter, A.; Szajkowski, L.; Werner, G.; Zhou, K. M.; Grigoriev, I. V.; Rokhsar, D. S.; Grossman, A. R.; Annotation, C.; Team, J. A. The *Chlamydomonas* genome reveals the evolution of key animal and plant functions. *Science* **2007**, *318* (5848), 245–251.

(25) Nguyen, A. V.; Thomas-Hall, S. R.; Malnoe, A.; Timmins, M.; Mussgnug, J. H.; Rupprecht, J.; Kruse, O.; Hankamer, B.; Schenk, P. M. Transcriptome for photobiological hydrogen production induced by sulfur deprivation in the green alga *Chlamydomonas reinhardtii*. *Eukaryotic Cell* **2008**, *7* (11), 1965–1979.

(26) Zhang, L. P.; Melis, A. Probing green algal hydrogen production. *Philos. Trans. R. Soc. Lond., Ser. B* **2002**, *357* (1426), 1499–1507.

(27) Chen, H. C.; Melis, A. Localization and function of SulP, a nuclear-encoded chloroplast sulfate permease in *Chlamydomonas reinhardtii*. *Planta* **2004**, *220* (2), 198–210.

(28) Deng, Z. P.; Zhang, X.; Tang, W. Q.; Oses-Prieto, J. A.; Suzuki, N.; Gendron, J. M.; Chen, H. J.; Guan, S. H.; Chalkley, R. J.; Peterman, T. K.; Burlingame, A. L.; Wang, Z. Y. A proteomics study of brassinosteroid response in *Arabidopsis*. *Mol. Cell. Proteomics* **2007**, *6* (12), 2058–2071.

(29) Griffin, T. J.; Gygi, S. P.; Ideker, T.; Rist, B.; Eng, J.; Hood, L.; Aebersold, R. Complementary profiling of gene expression at the transcriptome and proteome levels in *Saccharomyces cerevisiae*. *Mol. Cell. Proteomics* **2002**, *1* (4), 323–333.

(30) Ideker, T.; Thorsson, V.; Ranish, J. A.; Christmas, R.; Buhler, J.; Eng, J. K.; Bumgarner, R.; Goodlett, D. R.; Aebersold, R.; Hood, L. Integrated genomic and proteomic analyses of a systematically perturbed metabolic network. *Science* **2001**, *292* (5518), 929–934.

(31) Tian, Q.; Stepaniants, S. B.; Mao, M.; Weng, L.; Feetham, M. C.; Doyle, M. J.; Yi, E. C.; Dai, H. Y.; Thorsson, V.; Eng, J.; Goodlett, D.; Berger, J. P.; Gunter, B.; Linseley, P. S.; Stoughton, R. B.; Aebersold, R.; Collins, S. J.; Hanlon, W. A.; Hood, L. E. Integrated genomic and proteomic analyses of gene expression in mammalian cells. *Mol. Cell. Proteomics* **2004**, *3* (10), 960–969.

(32) Huber, M.; Bahr, I.; Kratzschmar, J. R.; Becker, A.; Muller, E. C.; Donner, P.; Pohlenz, H. D.; Schneider, M. R.; Sommer, A. Comparison of proteomic and genomic analyses of the human breast cancer cell line T47D and the antiestrogen-resistant derivative T47D-r. *Mol. Cell. Proteomics* **2004**, *3* (1), 43–55.

(33) Fulda, S.; Huang, F.; Nilsson, F.; Hagemann, M.; Norling, B. Proteomics of *Synechocystis* sp strain PCC 6803 - Identification of

periplasmic proteins in cells grown at low and high salt concentrations. *Eur. J. Biochem.* **2000**, *267* (19), 5900–5907.
(34) Huang, F.; Parmryd, I.; Nilsson, F.; Persson, A. L.; Pakrasi, H. B.; Andersson, B.; Norling, B. Proteomics of *Synechocystis* sp strain PCC 6803 - Identification of plasma membrane proteins. *Mol. Cell. Proteomics* **2002**, *1* (12), 956–966.
(35) Huang, F.; Hedman, E.; Funk, C.; Kieselbach, T.; Schroder, W. P.; Norling, B. Isolation of outer membrane of *Synechocystis* sp PCC 6803 and its proteomic characterization. *Mol. Cell. Proteomics* **2004**, *3* (6), 586–595.
(36) Herranen, M.; Battchikova, N.; Zhang, P. P.; Graf, A.; Sirpio, S.; Paakkarinen, V.; Aro, E. M. Towards functional proteomics of membrane protein complexes in *Synechocystis* sp PCC 6803. *Plant Physiol.* **2004**, *134* (1), 470–481.
(37) Wegener, K. M.; Welsh, E. A.; Thornton, L. E.; Keren, N.; Jacobs, J. M.; Hixson, K. K.; Monroe, M. E.; Camp, D. G.; Smith, R. D.; Pakrasi, H. B. High sensitivity proteomics assisted discovery of a novel operon involved in the assembly of photosystem II, a membrane protein complex. *J. Biol. Chem.* **2008**, *283* (41), 27829–27837.
(38) Zhang, L. F.; Yang, H. M.; Cui, S. X.; Hu, J.; Wang, J.; Kuang, T. Y.; Norling, B.; Huang, F. Proteomic analysis of plasma membranes of cyanobacterium *Synechocystis* sp strain PCC 6803 in response to high pH stress. *J. Proteome Res.* **2009**, *8* (6), 2892–2902.
(39) Rolland, N.; Atteia, A.; Decottignies, P.; Garin, J.; Hippler, M.; Kreimer, G.; Lemaire, S. D.; Mittag, M.; Wagner, V. *Chlamydomonas* proteomics. *Curr. Opin. Microbiol.* **2009**, *12* (3), 285–291.
(40) Hippler, M.; Klein, J.; Fink, A.; Allinger, T.; Hoerth, P. Towards functional proteomics of membrane protein complexes: analysis of thylakoid membranes from *Chlamydomonas reinhardtii*. *Plant J.* **2001**, *28* (5), 595–606.
(41) Turkina, M. V.; Kargul, J.; Blanco-Rivero, A.; Villarejo, A.; Barber, J.; Vener, A. V. Environmentally modulated phosphoproteome of photosynthetic membranes in the green alga *Chlamydomonas reinhardtii*. *Mol. Cell. Proteomics* **2006**, *5* (8), 1412–1425.
(42) Naumann, B.; Busch, A.; Allmer, J.; Ostendorf, E.; Zeller, M.; Kirchhoff, H.; Hippler, M. Comparative quantitative proteomics to investigate the remodeling of bioenergetic pathways under iron deficiency in *Chlamydomonas reinhardtii*. *Proteomics* **2007**, *7* (21), 3964–3979.
(43) Stauber, E. J.; Busch, A.; Naumann, B.; Svatos, A.; Hippler, M. Proteotypic profiling of LHCI from *Chlamydomonas reinhardtii* provides new insights into structure and function of the complex. *Proteomics* **2009**, *9* (2), 398–408.
(44) Yamaguchi, K.; Beligni, M. V.; Prieto, S.; Haynes, P. A.; McDonald, W. H.; Yates, J. R.; Mayfield, S. P. Proteomic characterization of the *Chlamydomonas reinhardtii* chloroplast ribosome - Identification of proteins unique to the 70 S ribosome. *J. Biol. Chem.* **2003**, *278* (36), 33774–33785.
(45) Schmidt, M.; Gessner, G.; Matthias, L.; Heiland, I.; Wagner, V.; Kaminski, M.; Geimer, S.; Eitzinger, N.; Reissenweber, T.; Voytsekh, O.; Fiedler, M.; Mittag, M.; Kreimer, G. Proteomic analysis of the eyespot of *Chlamydomonas reinhardtii* provides novel insights into its components and tactic movements. *Plant Cell* **2006**, *18* (8), 1908–1930.
(46) Wagner, V.; Ullmann, K.; Mollwo, A.; Kaminski, M.; Mittag, M.; Kreimer, G. The phosphoproteome of a *Chlamydomonas reinhardtii* eyespot fraction includes key proteins of the light signaling pathway. *Plant Physiol.* **2008**, *146* (2), 772–788.
(47) Pazour, G. J.; Agrin, N.; Leszyk, J.; Witman, G. B. Proteomic analysis of a eukaryotic cilium. *J. Cell Biol.* **2005**, *170* (1), 103–113.
(48) Gillet, S.; Decottignies, P.; Chardonnet, S.; Le Marechal, P. Cadmium response and redoxin targets in *Chlamydomonas reinhardtii*: a proteomic approach. *Photosynth. Res.* **2006**, *89* (2−3), 201–211.
(49) Lemaire, S. D.; Guillon, B.; Le Marechal, P.; Keryer, E.; Miginiac-Maslow, M.; Decottignies, P. New thioredoxin targets in the unicellular photosynthetic eukaryote *Chlamydomonas reinhardtii*. *Proc. Natl. Acad. Sci. U.S.A.* **2004**, *101* (19), 7475–7480.
(50) Michelet, L.; Zaffagnini, M.; Vanacker, H.; Le Marechal, P.; Marchand, C.; Schroda, M.; Lemaire, S. D.; Decottignies, P. In vivo targets of S-thiolation in *Chlamydomonas reinhardtii*. *J. Biol. Chem.* **2008**, *283* (31), 21571–21578.
(51) Gorman, D. S.; Levine, R. P. Cytochrome f and plastocyanin - Their sequence in photosynthetic electron transport chain of *Chlamydomonas reinhardii*. *Proc. Natl. Acad. Sci. U.S.A.* **1965**, *54* (6), 1665.
(52) Arnon, D. I. Copper enzymes in isolated chloroplasts - Polyphenoloxidase in beta-vulgaris. *Plant Physiol.* **1949**, *24* (1), 1–15.
(53) Cui, S. X.; Hu, J.; Yang, B.; Shi, L.; Huang, F.; Tsai, S. N.; Ngai, S. M.; He, Y. K.; Zhang, J. H. Proteomic characterization of *Phragmites communis* in ecotypes of swamp and desert dune. *Proteomics* **2009**, *9* (16), 3950–3967.
(54) Bradford, M. M. Rapid and sensitive method for quantitation of microgram quantities of protein utilizing principle of protein-dye binding. *Anal. Biochem.* **1976**, *72* (1−2), 248–254.
(55) Laemmli, U. K. Cleavage of structural proteins during assembly of head of bacteriophage-T4. *Nature* **1970**, *227* (5259), 680–685.
(56) Yang, P. F.; Li, X. J.; Wang, X. Q.; Chen, H.; Chen, F.; Shen, S. H. Proteomic analysis of rice (*Oryza sativa*) seeds during germination. *Proteomics* **2007**, *7* (18), 3358–3368.
(57) Emanuelsson, O.; Nielsen, H.; Brunak, S.; von Heijne, G. Predicting subcellular localization of proteins based on their N-terminal amino acid sequence. *J. Mol. Biol.* **2000**, *300* (4), 1005–1016.
(58) Zhou, J.; Zhou, J. X.; Yang, H. M.; Yan, C. S.; Huang, F. Characterization of a sodium-regulated glutaminase from cyanobacterium *Synechocystis* sp. PCC 6803. *Sci. China, Ser. C: Life Sci.* **2008**, *51* (12), 1066–1075.
(59) Zhou, J. X.; Zhou, J.; Yang, H. M.; Chen, M.; Huang, F. Characterization of two glutaminases from the filamentous cyanobacterium *Anabaena* sp PCC 7120. *FEMS Microbiol. Lett.* **2008**, *289* (2), 241–249.
(60) Kosourov, S.; Tsygankov, A.; Seibert, M.; Ghirardi, M. L. Sustained hydrogen photoproduction by *Chlamydomonas reinhardtii*: effects of culture parameters. *Biotechnol. Bioeng.* **2002**, *78* (7), 731–740.
(61) Hemschemeier, A.; Melis, A.; Happe, T. Analytical approaches to photobiological hydrogen production in unicellular green algae. *Photosynth. Res.* **2009**, *102* (2−3), 523–540.
(62) Hemschemeier, A.; Happe, T. The exceptional photofermentative hydrogen metabolism of the green alga *Chlamydomonas reinhardtii*. *Biochem. Soc. Trans.* **2005**, *33*, 39–41.
(63) Makarova, V. V.; Kosourov, S.; Krendeleva, T. E.; Semin, B. K.; Kukarskikh, G. P.; Rubin, A. B.; Sayre, R. T.; Ghirardi, M. L.; Seibert, M. Photoproduction of hydrogen by sulfur-deprived *C. reinhardtii* mutants with impaired photosystem II photochemical activity. *Photosynth. Res.* **2007**, *94* (1), 79–89.
(64) Tsygankov, A.; Kosourov, S.; Seibert, M.; Ghirardi, M. L. Hydrogen photoproduction under continuous illumination by sulfur-deprived, synchronous *Chlamydomonas reinhardtii* cultures. *Int. J. Hydrogen Energy* **2002**, *27* (11−12), 1239–1244.
(65) Wessel, D.; Flugge, U. I. A method for the quantitative recovery of protein in dilute-solution in the presence of detergents and lipids. *Anal. Biochem.* **1984**, *138* (1), 141–143.
(66) Hurkman, W. J.; Tanaka, C. K. Solubilization of plant membrane-proteins for analysis by two-dimensional gel-electrophoresis. *Plant Physiol.* **1986**, *81* (3), 802–806.
(67) Granier, F. Extraction of plant-proteins for two-dimensional electrophoresis. *Electrophoresis* **1988**, *9* (11), 712–718.
(68) Forster, B.; Mathesius, U.; Pogson, B. J. Comparative proteomics of high light stress in the model alga *Chlamydomonas reinhardtii*. *Proteomics* **2006**, *6* (15), 4309–4320.
(69) HarrisE. H. *The Chlamydomonas Sourcebook: A Comprehensive Guide to Biology and Laboratory Use*; Academic Press: San Diego, CA, 1989.
(70) May, P.; Wienkoop, S.; Kempa, S.; Usadel, B.; Christian, N.; Rupprecht, J.; Weiss, J.; Recuenco-Munoz, L.; Ebenhoh, O.; Weckwerth, W.; Walther, D. Metabolomics- and proteomics-assisted genome annotation and analysis of the draft metabolic network of *Chlamydomonas reinhardtii*. *Genetics* **2008**, *179* (1), 157–166.
(71) De Las Rivas, J.; Balsera, M.; Barber, J. Evolution of oxygenic photosynthesis: genome-wide analysis of the OEC extrinsic proteins. *Trends Plant Sci.* **2004**, *9* (1), 18–25.
(72) Shutova, T.; Klimov, V. V.; Andersson, B.; Samuelsson, G. A cluster of carboxylic groups in PsbO protein is involved in proton transfer from the water oxidizing complex of Photosystem II. *Biochim. Biophys. Acta* **2007**, *1767* (6), 434–440.
(73) Roose, J. L.; Wegener, K. M.; Pakrasi, H. B. The extrinsic proteins of photosystem II. *Photosynth. Res.* **2007**, *92* (3), 369–387.
(74) Manuell, A. L.; Yamaguchi, K.; Haynes, P. A.; Milligan, R. A.; Mayfield, S. P. Composition and structure of the 80 S ribosome from the green alga *Chlamydomonas reinhardtii*: 80 S ribosomes are conserved in plants and animals. *J. Mol. Biol.* **2005**, *351* (2), 266–279.
(75) Schroda, M. The *Chlamydomonas* genome reveals its secrets: chaperone genes and the potential roles of their gene products in the chloroplast. *Photosynth. Res.* **2004**, *82* (3), 221–240.
(76) Harris, E. H. *The Chlamydomonas Sourcebook (Second Edition): Organellar and Metabolic Processes*; Academic Press: San Diego, CA, 2009.

(77) Drzymalla, C.; Schroda, M.; Beck, C. F. Light-inducible gene HSP70B encodes a chloroplast-localized heat-shock protein in *Chlamydomonas reinhardtii*. *Plant Mol. Biol.* **1996**, *31* (6), 1185–1194.
(78) Atteia, A.; Adrait, A.; Brugiere, S.; Tardif, M.; van Lis, R.; Deusch, O.; Dagan, T.; Kuhn, L.; Gontero, B.; Martin, W.; Garin, J.; Joyard, J.; Rolland, N. A proteomic survey of *Chlamydomonas reinhardtii* mitochondria sheds new light on the metabolic plasticity of the organelle and on the nature of the alpha-proteobacterial mitochondrial ancestor. *Mol. Biol. Evol.* **2009**, *26* (7), 1533–1548.
(79) Liu, C. M.; Willmund, F.; Whitelegge, J. P.; Hawat, S.; Knapp, B.; Lodha, M.; Schroda, M. J-domain protein CDJ2 and HSP70B are a plastidic chaperone pair that interacts with vesicle-inducing protein in plastids 1. *Mol. Biol. Cell* **2005**, *16* (3), 1165–1177.
(80) Srivastava, R.; Pisareva, T.; Norling, B. Proteomic studies of the thylakoid membrane of *Synechocystis* sp PCC 6803. *Proteomics* **2005**, *5* (18), 4905–4916.
(81) Westphal, S.; Heins, L.; Soll, J.; Vothknecht, U. C. Vipp1 deletion mutant of *Synechocystis*: a connection between bacterial phage shock and thylakoid biogenesis. *Proc. Natl. Acad. Sci. U.S.A.* **2001**, *98* (7), 4243–4248.
(82) Schroda, M.; Vallon, O.; Whitelegge, J. P.; Beck, C. F.; Wollman, F. A. The chloroplastic GrpE homolog of *Chlamydomonas*: two isoforms generated by differential splicing. *Plant Cell* **2001**, *13* (12), 2823–2839.
(83) van Lis, R.; Atteia, A.; Mendoza-Hernandez, G.; Gonzalez-Halphen, D. Identification of novel mitochondrial protein components of *Chlamydomonas reinhardtii*. A proteomic approach. *Plant Physiol.* **2003**, *132* (1), 318–330.
(84) Edvardsson, A.; Shapiguzov, A.; Petersson, U. A.; Schroder, W. P.; Vener, A. V. Immunophilin AtFKBP13 sustains all peptidyl-prolyl isomerase activity in the thylakoid lumen from *Arabidopsis thaliana* deficient in AtCYP20-2. *Biochemistry* **2007**, *46* (33), 9432–9442.
(85) Yano, M.; Koumoto, Y.; Kanesaki, Y.; Wu, X. J.; Kido, H. 20S proteasorne prevents aggregation of heat-denatured proteins without PA700 regulatory subcomplex like a molecular chaperone. *Biomacromolecules* **2004**, *5* (4), 1465–1469.
(86) Schreiner, O.; Lien, T.; Knutsen, G. Capacity for arylsulfatase synthesis in synchronous and synchronized cultures of *Chlamydomonas reinhardtii*. *Biochim. Biophys. Acta* **1975**, *384* (1), 180–193.
(87) De hostos, E. L.; Togasaki, R. K.; Grossman, A. Purification and biosynthesis of a derepressible periplasmic arylsulfatase from *Chlamydomonas reinhardtii*. *J. Cell Biol.* **1988**, *106* (1), 29–37.
(88) De hostos, E. L.; Schilling, J.; Grossman, A. R. Structure and expression of the gene encoding the periplasmic arylsulfatase of *Chlamydomonas reinhardtii*. *Mol. Gen. Genet.* **1989**, *218* (2), 229–239.
(89) Takahashi, H.; Braby, C. E.; Grossman, A. R. Sulfur economy and cell wall biosynthesis during sulfur limitation of *Chlamydomonas reinhardtii*. *Plant Physiol.* **2001**, *127* (2), 665–673.
(90) Florencio, F. J.; Vega, J. M. Separation, purification, and characterization of 2 isoforms of glutamine-synthetase from *Chlamydomonas reinhardii*. *Z. Naturforsch.* **1983**, *38* (7−8), 531–538.
(91) Fischer, P.; Klein, U. Localization of nitrogen-assimilating enzymes in the chloroplast of *Chlamydomonas reinhardtii*. *Plant Physiol.* **1988**, *88* (3), 947–952.
(92) Chen, Q.; Silflow, C. D. Isolation and characterization of glutamine synthetase genes in *Chlamydomonas reinhardtii*. *Plant Physiol.* **1996**, *112* (3), 987–996.

PR100076C